CHAPTER II
THEORETICAL BACKGROUND AND LITERATURE REVIEW

2.1 Background

At present, an increasing of energy problems stimulated many people to realize for the changing of our world. To cope with this problem, many researchers try to find the new energy sources for compensated the decreasing of fossil fuels. Among the various sources of energy, Hydrogen has attracted much attention because it provides clean energy which is environmentally friendly. Nevertheless, it can be produced from both renewable and non-renewable sources (Bičáková and Straka, 2012). PEMFCs were recommended to produce clean energy by converting hydrogen for mobile power application due to low operating temperature about 80 °C (Ghenciu, 2002). The ideal fuel for PEMFCs is hydrogen, which is stored for on-board applications by several types such as gas compressed, liquid, and hydrogen storage materials. However, the cost of these types is expensive because it required a specific filling station infrastructure. So, methanol became a promising source of hydrogen for PEMFCs due to its easy availability, low processing temperature, low contaminant level, and safe in handling (Ahmed and Krumpelt, 2001). In addition, hydrogen can be converted from methanol into hydrogen by several reactions, which differed from each other (Ou *et al.*, 2008). The selected reaction depended on an application that was applied.

2.2 Hydrogen Production from Methanol (CH_3OH)

As previously mentioned, hydrogen is a promising candidate because it can be produced from both renewable and non-renewable sources, as shown in Figure 2.1. Moreover, it provided energy which was environmentally friendly as compared to fossil fuel. So, it may reduce the topic that concerned about global warming and ecological problems.

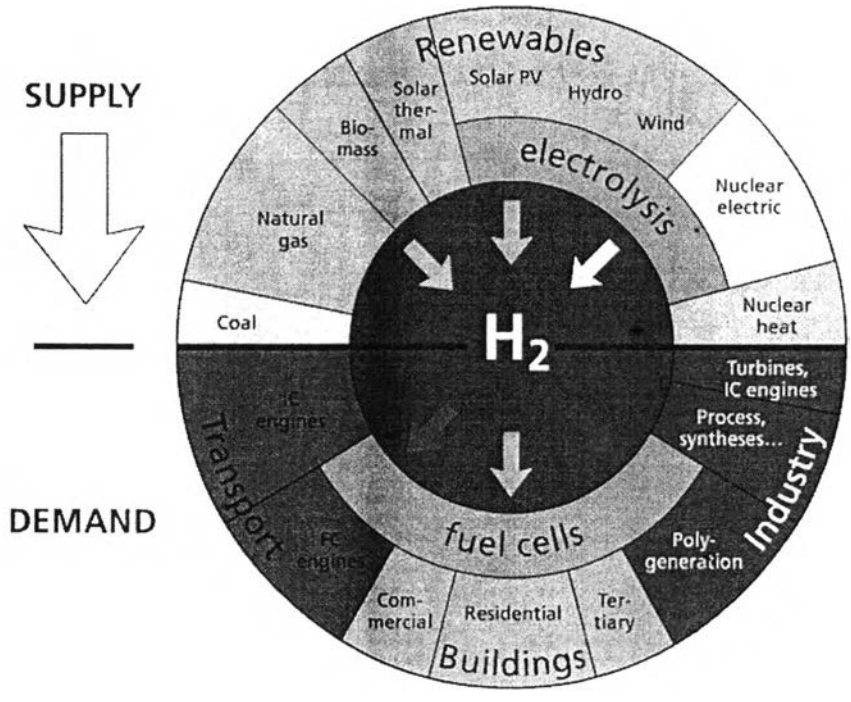

Figure 2.1 Hydrogen: primary energy sources, energy converters and applications (Source: http://ec.europa.eu/research/energy/pdf/hydrogen-report_en.pdf).

PEMFCs are suitable power generation devices that converted hydrogen to energy for mobile applications. However, hydrogen is difficult to store and transport (Sá *et al.*, 2010). If they need to use hydrogen for on board storage in the vehicle, including hydrogen storage materials, liquid, and gas compressed, an expensive infrastructure would require for building a specific filling station. The hydrogen storage in form of liquid fuels was become an attractive route because it can eliminate the problem that occurred before. The main advantage of liquid fuels is their high energy density, ease of handling, and inexpensive. Moreover, it can be used for the on-demand production of hydrogen for fuel cells, with applications in mobile and stationary grid-dependent power systems (Pérez-Hernández *et al.*, 2008). Figure 2.2 shows the efficiency of liquid fuels as a function of H/C atomic ratio. Among the various types of liquid fuel, methanol is a prominent candidate because it can be catalytically reformed into an H_2-rich gas at moderate temperature (200-400 °C) that occurred at comparatively lower temperature as compared to the temperature

(800–900 °C) for gasoline reforming. There are several processes that used to produce hydrogen by using methanol as a hydrogen source such as steam reforming (SRM), partial oxidation (POM), methanol decomposition (DM), and oxidative steam reforming (OSRM) (Hong and Ren, 2008).

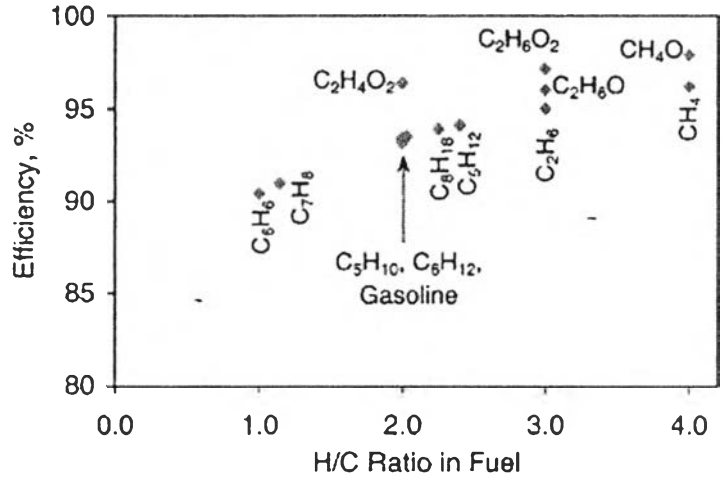

Figure 2.2 The effect of the hydrogen-to-carbon atomic ratio in the fuel on the theoretical fuel processing efficiency (Ahmed and Krumpelt, 2001).

2.2.1 Steam Reforming of Methanol (SRM)

Steam reforming is a common reactions that used to produce hydrogen from hydrocarbon. This reaction is an endothermic reaction. Hence, the reaction required energy input and high temperature for operation (Liu *et al.*, 2003). Moreover, this reaction has attracted much attention as a potential technology to apply for PEMFCs (Sá *et al.*, 2010). The reaction for steam reforming of methanol is considered as :

$$CH_3OH + H_2O \rightarrow CO_2 + 3H_2 \qquad \Delta H^{o}_{298} = +49.4\ kJmol^{-1} \qquad (2.1)$$

The steam reforming of methanol (SRM) has the highest yield of hydrogen and the selectivity to CO_2 from SRM can be very high, depending on the

type of catalysts. The SRM reaction is a sequence of the methanol decomposition (DM) reaction and water gas shift (WGS) reaction (Zhang and Shi, 2003).

$$CH_3OH \rightarrow CO + H_2 \qquad \Delta H^0_{298} = +92.0\ kJmol^{-1} \qquad (2.2)$$

$$CO + H_2O \rightarrow CO_2 + H_2 \qquad \Delta H^0_{298} = -41.1\ kJmol^{-1} \qquad (2.3)$$

Normally, the steam reforming process is usually operated with excess steam which induced the WGS reaction in order to reduce the amount of CO formation in the product stream. For the hydrogen to be used in the PEMFCs, CO is a poison because CO can deteriorate a Pt-electrode and reduce performance of PEM fuel cells. To reduce the amount of CO (<10 ppm), the processes such as high-temperature and low-temperature water gas shift, and preferential CO oxidation were used to follow the process of steam reforming (Huang and Chen, 2010).

The steam reforming of methanol can also lead to the formation of toxic and undesirable product such as formaldehyde (CH_2O), formic acid (HCOOH), methyl formate ($HCOOCH_3$) and dimethylether (CH_3OCH_3), which limit the hydrogen (Houteit *et al.*, 2006). The different reaction pathways are shown in Figure 2.3. Moreover, methane (CH_4) was observed as a by-product which depended on the type of catalyst and the operating conditions. The formation of methane consumes hydrogen from methanol and steam that suppressed the production of hydrogen, as shown in Equation 2.4.

$$CO(g) + 3H_2(g) \rightarrow CH_4(g) + H_2O(g) \qquad \Delta H^0_{298} = -206\ kJmol^{-1} \qquad (2.4)$$

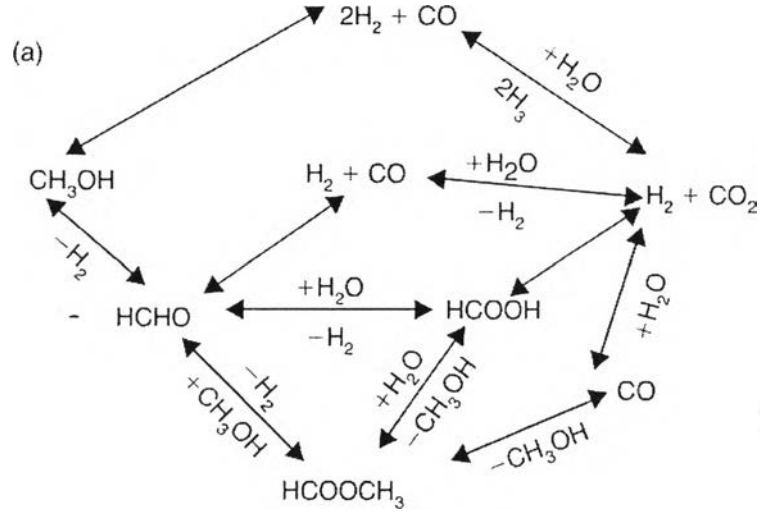

Figure 2.3 The different reaction pathways for SRM reaction (Kundu *et al.*, 2007).

Both CO and CH_4 that produced in steam reforming reaction are a source of coke formation which lead to the deactivation of catalyst. There are two main pathways for coke (carbon) formation (Armor, 1999) :

$$2CO \rightarrow CO_2 + C \qquad (2.5)$$

$$CH_4 \rightarrow C + 2H_2 \qquad (2.6)$$

2.2.1.1 Experimental Condition

The effect of reaction temperature on gas product distribution is shown in Figure 2.4. The methanol conversion exhibited typical S-shaped temperature dependence. The production of H_2 and CO_2 increased as the temperature increased and were produced about 3:1 ratio. CO formation is initiated at 300 °C.

The effect of H_2O/CH_3OH molar ratio is shown in Figure 2.5. The result showed that methanol conversion increases with increasing the H_2O/CH_3OH molar ratio. When H_2O/CH_3OH was increased greater than 1.0, an increase in methanol conversion slows down, and hydrogen yield also increases slowly. In term of outlet CO concentration, this concentration decreased to 0.1 mol% with increasing H_2O/CH_3OH molar ratio up to 1.5. Therefore, it indicated that higher H_2O/CH_3OH molar ratio was favorable for reducing the outlet CO concentration due

to the enhancement of WGS reaction. This can be explained by Equations (2.1)-(2.3). Excess H_2O promoted methanol conversion and reduced CO concentration by shifting the equilibrium to right side.

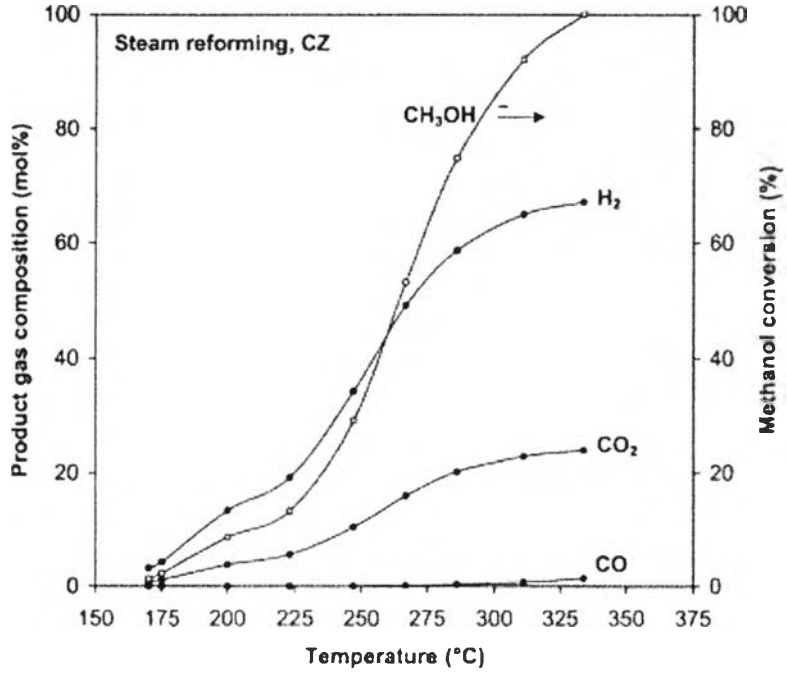

Figure 2.4 Product gas composition and methanol conversion versus reaction temperature during steam reforming of methanol over catalyst CZ (Agrell *et al.*, 2003).

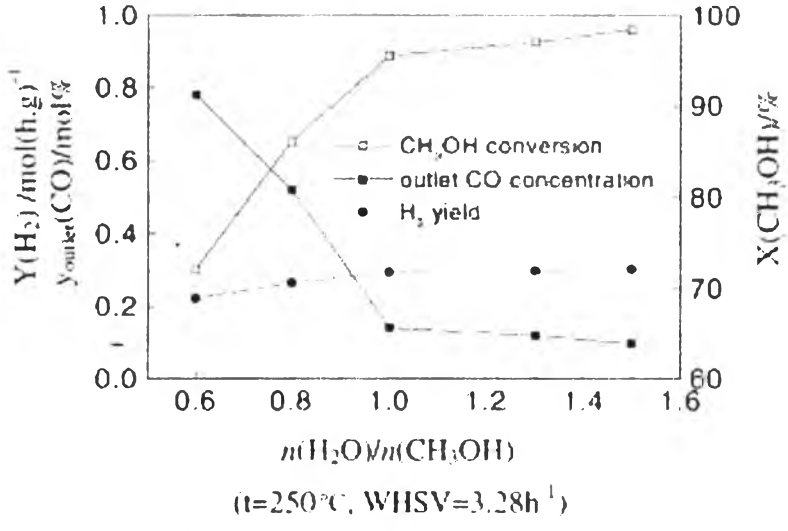

Figure 2.5 Effect of H_2O/CH_3OH molar ratio on catalytic activity (Zhang and Shi, 2003).

Zhang and Shi (2003) studied the effect of methanol space velocity (WHSV) to the catalytic activity of steam reforming of methanol. The result showed that as methanol space velocity increased, methanol conversion and the outlet CO concentration decreased, and hydrogen yield has a maximum in this experiment conditions. However, methanol space velocity does not influence the selectivity of H_2 which remained around 99.9% throughout the experiment.

2.2.1.2 Mechanism and Kinetics of Methanol Steam Reforming

The mechanism of steam reforming of methanol is still debated. So, the kinetic studies and reaction mechanisms data are limited. Some researchers proposed the reaction sequence of methanol steam decomposition followed by water gas shift reaction (WGS), as shown in Equations (2.7)-(2.8) (Santacesaria and Carrá, 1983).

$$CH_3OH \leftrightarrow 2H_2 + CO \qquad \Delta H^0_{298} = +91.0 \text{ kJmol}^{-1} \qquad (2.7)$$

$$CO + H_2 \leftrightarrow CO_2 + H_2 \qquad \Delta H^0_{298} = -41.0 \text{ kJmol}^{-1} \qquad (2.8)$$

The carbon monoxide is produced first. Hence, its concentration in the product stream must be equal to or greater than the concentration of CO at the WGS reaction equilibrium. The elemental surface reaction mechanisms were proposed and derived the Langmiur-Hinshelwood expression by (Jiang *et al.*, 1993; Jiang *et al.*, 1993). They suggested CO formation via decomposition of methyl formate (Equations 2.9-2.11).

$$CH_3OH \rightarrow CH_3OCHO + 2H_2 \quad (2.9)$$

$$CH_3OCHO + H_2O \rightarrow HCOOH + CH_3OH \quad (2.10)$$

$$HCOOH \rightarrow CO_2 + H_2 \quad (2.11)$$

This kinetic expression can use to predict the rates of methanol conversion and carbon dioxide formation. They neglect the CO formation that cannot be neglected as even very low CO concentration can poison the Pt anode of PEM fuel cell. To investigate the CO formation mechanism, DRIFT analysis was used to study. They confirmed that the CO formation over $CuO/ZnO/ZrO_2/Al_2O_3$ catalyst for SRM occurs via reverse water gas shift reaction (rWGS) (Equation 2.12) (Breen and Ross, 1999). Lately, many researchers also proposed the CO formation via rWGS that used the products of the reforming reaction such as H_2, and CO_2.

$$CO_2 + H_2 \leftrightarrow CO + H_2O \qquad \Delta H^o_R = +41 \text{ kJmol}^{-1} \quad (2.12)$$

The kinetics of catalytic SRM was studied by using $CuO/ZnO/Al_2O_3$ catalyst. SRM and DM reactions can be considered irreversible for generating a semi-empirical model of catalytic SRM. They found that the WGS reaction could be neglected without a substantial loss in accuracy. The rate constants that used for developing the model were k_1 (SRM reaction), and k_2 (DM reaction). The rate equations can be written as the following equations:

$$r_{CH3OH} = -k_1C_{CH3OH} - k_2$$

$$r_{H2O} = -k_1C_{CH3OH}$$

$$r_{CO2} = k_1C_{CH3OH}$$

$$r_{CO} = k_2$$

$$r_{H2} = 3k_1C_{CH3OH} + 2k_2$$

The rate constants k_1 and k_2 are both functions of temperature and pressure. The reaction rate of methanol and water consumption only depended on the concentration of methanol not water concentration. For the rate production of CO, this reaction is affected slightly by the concentration of methanol or water. So, the order of this reaction is a zero-order (Amphlett *et al.*, 1994).

2.2.2 Partial Oxidation of Methanol (POM)

Partial oxidation of methanol is an exothermic reaction that occurred in the presence of air (oxygen). The POM reaction has a higher reaction rate than SRM and also provided a fast response to transient. Nevertheless, the temperature control of this reaction can be difficult due to its highly exothermic. Moreover, it can produce H_2 lower than SRM reaction (Kundu *et al.*, 2007). The reaction of POM is shown in Equation 2.13 and Figure 2.6.

$$CH_3OH(g) + (1/2)O_2(g) \rightarrow 2H_2(g) + CO_2(g) \quad \Delta H^{o}_{298} = -192.2\ kJmol^{-1} \quad (2.13)$$

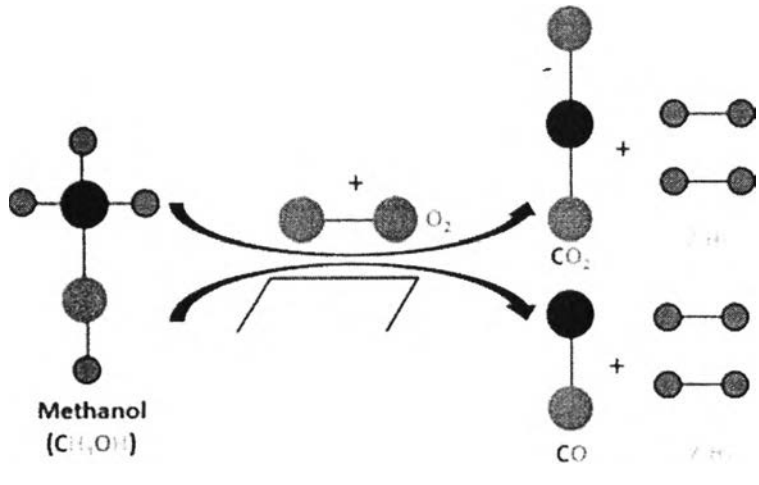

Figure 2.6 Reaction mechanism of POM (Qayyum *et al.*, 2012).

Many catalysts have been used in POM such as supported Cu, Pd, Pt, and Au. Copper-Zinc-supported gold catalysts gave higher hydrogen selectivity and lower carbon monoxide selectivity (Huang *et al.*, 2011).

However, a number of other reactions can take place during POM reaction. These reactions are mainly methanol oxidation, methanol decomposition, steam reforming, WGS reaction, methanation, CO oxidation, and H_2 oxidation. These are shown in Equations (2.14)-(2.20) (Ubago-Pérez *et al.*, 2007).

$$CH_3OH + 3/2O_2 \leftrightarrow CO_2 + 2H_2O \quad (2.14)$$

$$CH_3OH \leftrightarrow CO + 2H_2 \quad (2.15)$$

$$CH_3OH + H_2O \leftrightarrow 3H_2 + CO_2 \quad (2.16)$$

$$CO + H_2O \leftrightarrow CO_2 + H_2 \quad (2.17)$$

$$CO + 3H_2 \leftrightarrow CH_4 + H_2O \quad (2.18)$$

$$CO + 1/2O_2 \leftrightarrow CO_2 \quad (2.19)$$

$$H_2 + 1/2O_2 \leftrightarrow H_2O \quad (2.20)$$

From the above reactions, methanol decomposition can produce CO that deteriorated a Pt electrode and reduced the efficiency of PEMFCs.

2.2.2.1 Experimental Condition

The effect of reaction temperature was studied at reaction temperature between 200 and 325 °C by using Au–Cu/TiO_2 as a catalyst (Figure 2.7). When the temperature increased, the CH_3OH conversion and H_2 selectivity increased from 80.4 to 99.6% and 73.4 to 98%, respectively. The O_2 conversion was 95.5% at 200 °C and increased to 99.5% at 325 °C. However, the CO selectivity significantly increased at 275 °C. This indicated that when the reaction temperature ≥ 275 °C, the unfavorable reactions such as methanol decomposition, and Reverse water gas shift (rWGS) occurred. Moreover, the significant amount of CO at high temperature implied that the reaction rate of methanol decomposition is faster than CO oxidation and WGS reaction.

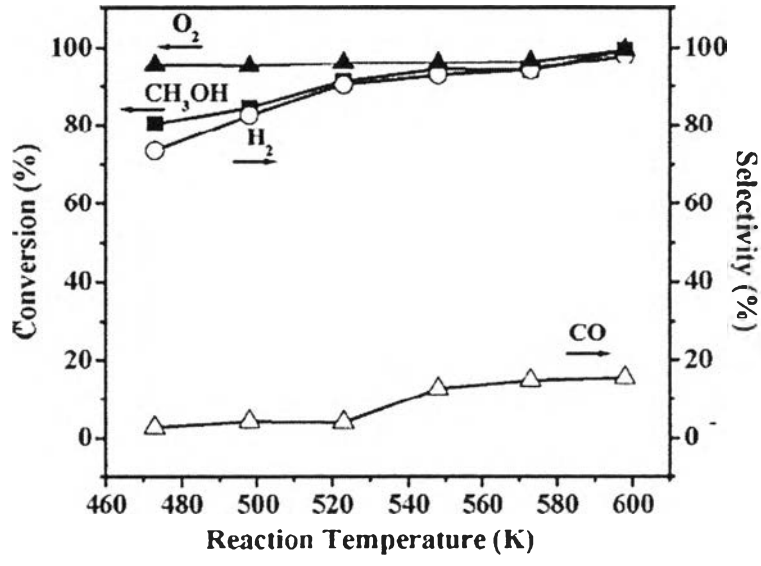

Figure 2.7 Effect of reaction temperature on CH_3OH conversion, O_2 conversion, H_2 selectivity and CO selectivity for POM reaction *(Ou et al., 2008)*.

The effect of oxygen/methanol ratios (O/M) was studied in various conditions at 200 °C by using gold on copper–zinc oxides catalyst. This study is shown in Figure. 2.8. When the O/M ratio is lower than 0.5, low methanol conversion was observed due to the stoichiometric inadequacy for POM reaction and kinetically insufficient for the decomposition of methanol. The methanol conversion increased to more than 95% as the O/M ration increased to 0.5 or higher. The increasing of O/M ratio also affected to H_2 selectivity. At low O/M ratio, the high H_2 selectivity was observed, but it decreased sharply with increasing O/M ratio. In term of CO selectivity, gold-deposited Copper–Zinc oxides (CZ) catalyst enhanced the CO selectivity by decreasing CO formation. Even though, the increasing of O/M ratio can reduce the initiation temperature and suppress CO formation, the side reactions cannot be neglected.

$Au/ZnO/Al_2O_3$ was used to test the catalytic activity of POM reaction under various calcination temperatures (Figure 2.9). Methanol conversion and hydrogen selectivity decreased as the calcination temperature increased. For H_2 selectivity, it showed the large difference at different calcination temperatures. The catalyst calcined at 600 °C showed negligible activity for hydrogen production.

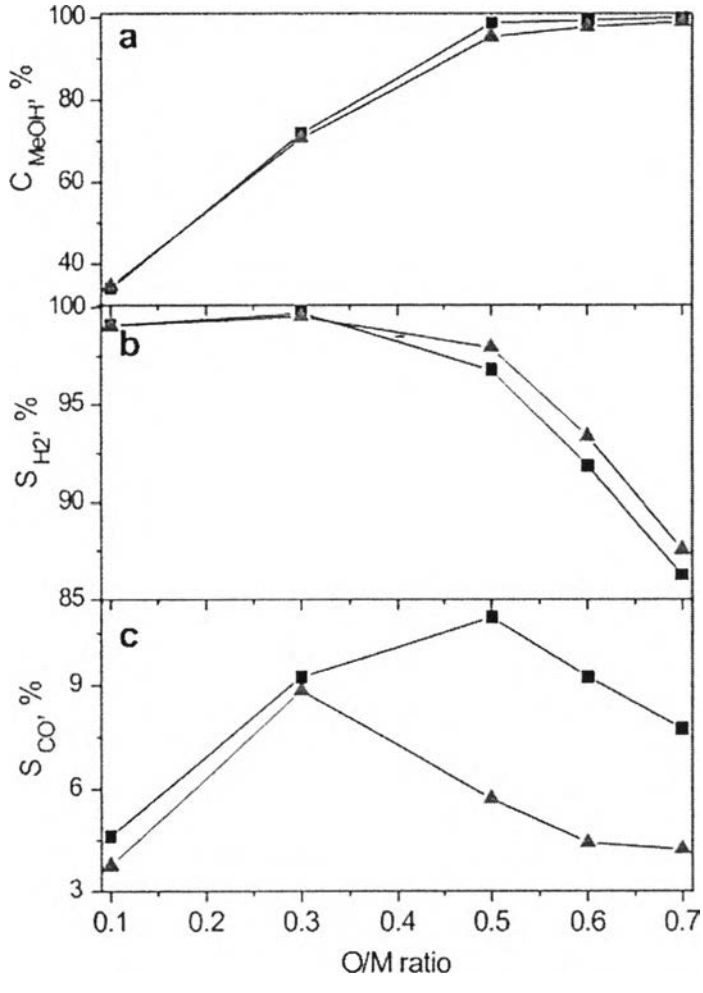

Figure 2.8 The performance of (■) Copper–Zinc oxides (CZ), (▲) $Au_{4.3}CZ$ in various O/M ratio of POM reaction at 200 °C (a) Methanol conversion; (b) Hydrogen selectivity; (c) Carbon monoxide selectivity (Huang *et al.*, 2011).

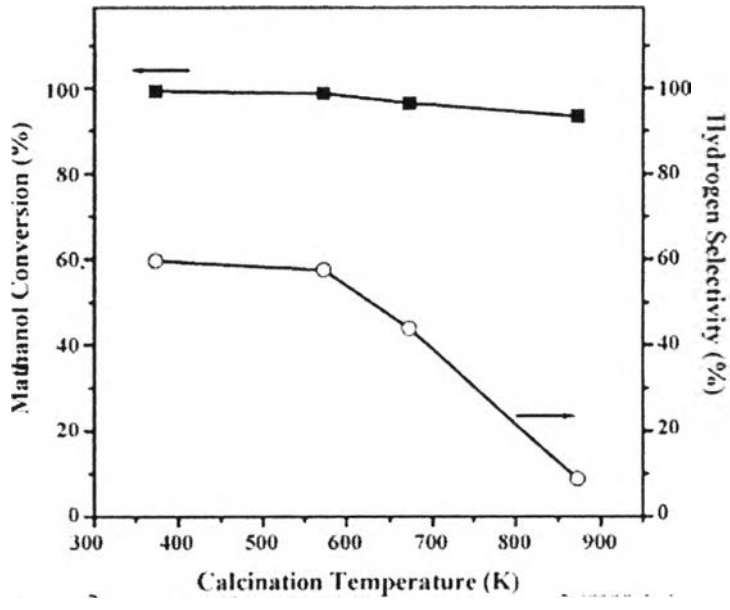

Figure 2.9 Effect of calcination temperature in methanol conversion and hydrogen selectivity for POM over $Au/ZnO/Al_2O_3$ catalyst (Chang *et al.*, 2008).

2.2.3 Oxidative Steam Reforming of Methanol (OSRM)

Oxidative steam reforming or Autothermal reforming is a combination of steam reforming and partial oxidation which fed air and steam together. The OSRM reaction utilized the heat generated from partial oxidation reaction to promote the endothermic steam reforming reaction. So, it can be run adiabatically. Moreover, this reaction generated relatively high hydrogen concentrations at moderate response rates and reduced the formation of CH_4, CO, and coke (Haynes and Shekhawat, 2011). The equation for OSRM reaction is

$$CH_3OH_{(g)} + (1\text{-}p)H_2O_{(g)} + 0.5pO_{2(g)} \rightarrow (3\text{-}p)H_{2(g)} + CO_{2(g)} \qquad (2.21)$$

$$\Delta H^{o}_{298} = -241.8p + 49.5 \text{ kJmol}^{-1}$$

The overall heat of reaction depended on the value of p, which directly influenced the thermal properties of OSRM system as well as hydrogen concentration (Patel and Pant, 2007).

The OSRM reaction generated not only CO_2 and H_2 but also CO, CH_4, formaldehyde (CH_2O), and dimethyl ether (DME), as shown in Figure 2.10. The formation of CH_4 can be explained by the higher methanol conversion which led to lower the H_2O concentrations. The unfavorable effect of steam on CO production is reduced under these conditions. So, CO can be formed and converted to CH_4 due to the high concentration of H_2. For CH_2O, it can be produced via methanol dehydrogenation and oxidative dehydrogenation reactions.

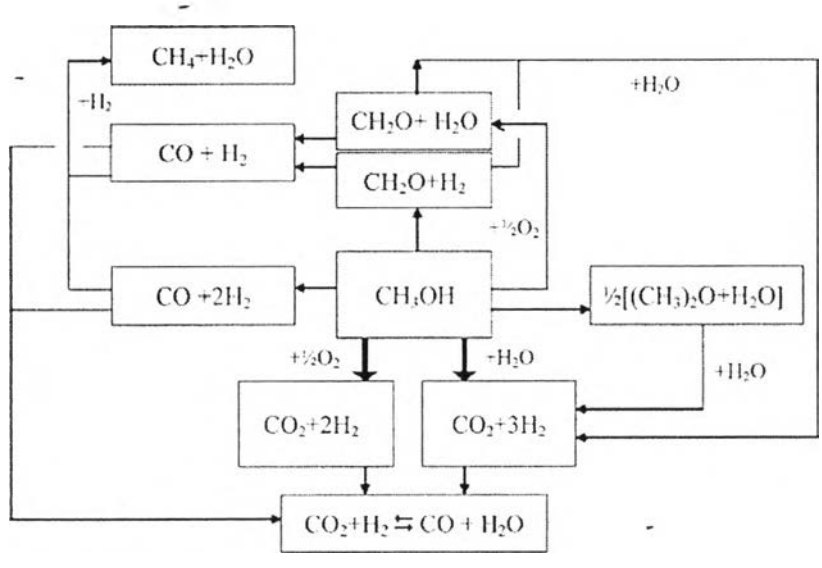

Figure 2.10 Reaction network under OSRM reactions (Turco *et al.*, 2004).

2.2.3.1 Experimental Condition

The effect of temperature on catalytic activity of OSRM reaction was tested on 2-Cu/Zn/Al (Figure 2.11). The methanol conversion increased as the temperature increased and reached to 90% at 400 °C. H_2 yield appeared negligible at low temperature and reached to 2 at 400 °C. This research also reported the conversion of methanol to different products. This result shows that the conversion to CO_2 is negligible at low temperature while the conversion of C_xH_yO increased. It was explained by the prevailing of the methanol dehydration and/or dehydrogenation reactions under these conditions. As the temperature increased to higher conditions, CO_2 conversion significantly increased to a value about 80% at 400 °C. In term of

C_xH_yO conversion, this conversion reached to a maximum value at 350 °C, and sharply decreased at 400 °C. CH_4 was formed in an appreciable amount at 400 °C. CO was not observed in all temperatures due to its concentration which is lower than the detection limit.

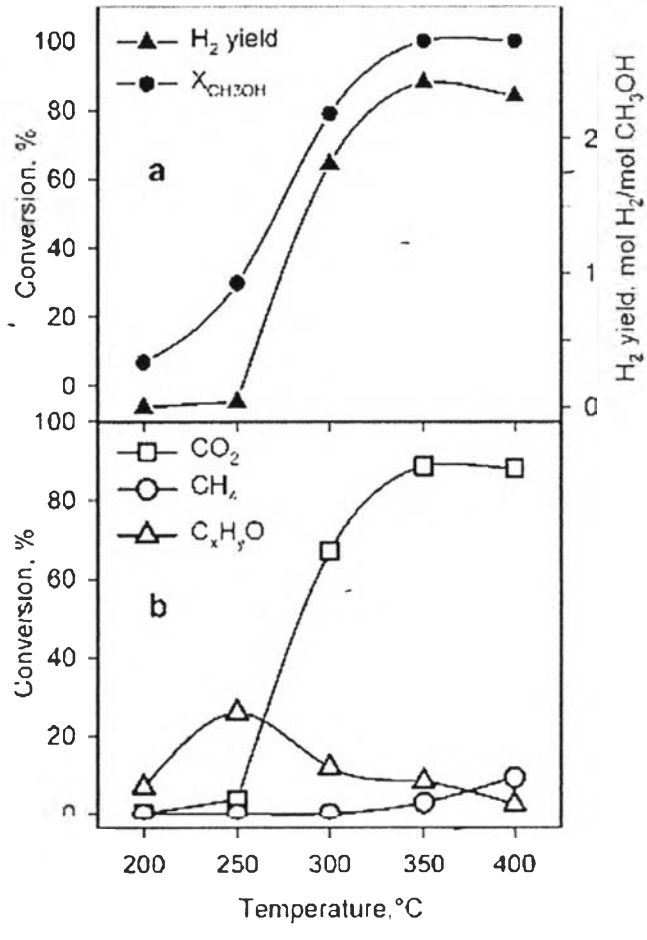

Figure 2.11 (a) Methanol conversion and hydrogen yield; (b) conversions to different products as a function of temperature under OSRM conditions for the catalyst 2-Cu/Zn/Al, GHSV = 0.6×10^5 h^{-1} (Turco *et al.*, 2004).

The effect of oxygen to methanol (O/M) molar ratio was demonstrated over Cu(20)CeAl catalyst (Figure 2.12). The methanol conversion and hydrogen production rate increased as the O/M molar ratio increased up to 0.15. Then, these values decreased with the increasing of O/M molar ratio. The hydrogen production rate decreased rapidly beyond O/M = 0.2 because of the POM reaction

which produced 2 mols of hydrogen per one mol of methanol reacted. When the O/M molar ratio increased, the formation of CO also increased from 0.13 mol% to 21.34 mol% at O/M = 0.5 which may be due to the decomposition of methanol.

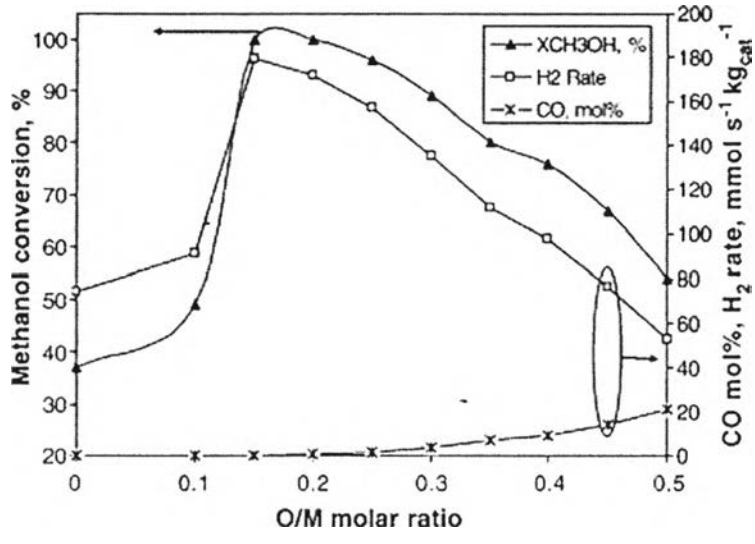

Figure 2.12 Effect of oxygen to methanol molar ratio over methanol conversion, hydrogen rate and carbon monoxide formation for Cu(20)CeAl catalyst, (W/F = 15 $kg_{cat}s\ mol^{-1}_{methanol}$, T = 280 °C, S/M = 1.5, P = 1 atm) (Patel and Pant, 2007).

The effect of copper loading on hydrogen selectivity was studied by using Cu/CeO_2 catalyst (Figure 2.13). The 2Cu sample showed the best H_2 selectivity up to 230 °C, after this temperature the 6Cu became the best catalyst that gave the highest value of H_2 selectivity. At the maximum reaction temperature which consumed all of methanol, the final products were H_2, CO_2, and H_2O. The H_2 depletion in 2Cu catalyst can be explained by the loss of active copper phase for H_2 generation.

The CO level over Cu/ZnO catalyst between steam reforming of methanol (SRM) and combined reforming of methanol (CRM) are shown in Figure 2.14. The CO formation over this catalyst is less pronounced during CRM than SRM reaction.

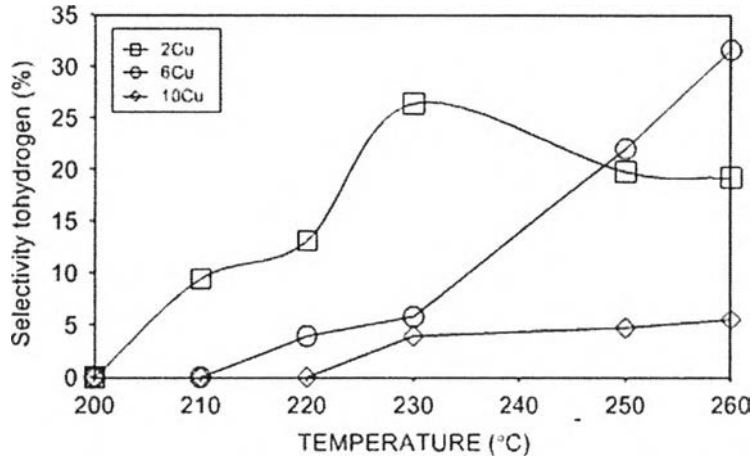

Figure 2.13 H_2 selectivity as a function of reaction temperature. $\%S(H_2)$ = $mol(H_2)/(mol(H_2+CO_2))*Xa$; $\%S(CO_2)$ = $mol(CO_2)/(mol(H_2+CO_2))*Xa$; Xa = %methanol conversion (mol%) (Pérez-Hernández *et al.*, 2007).

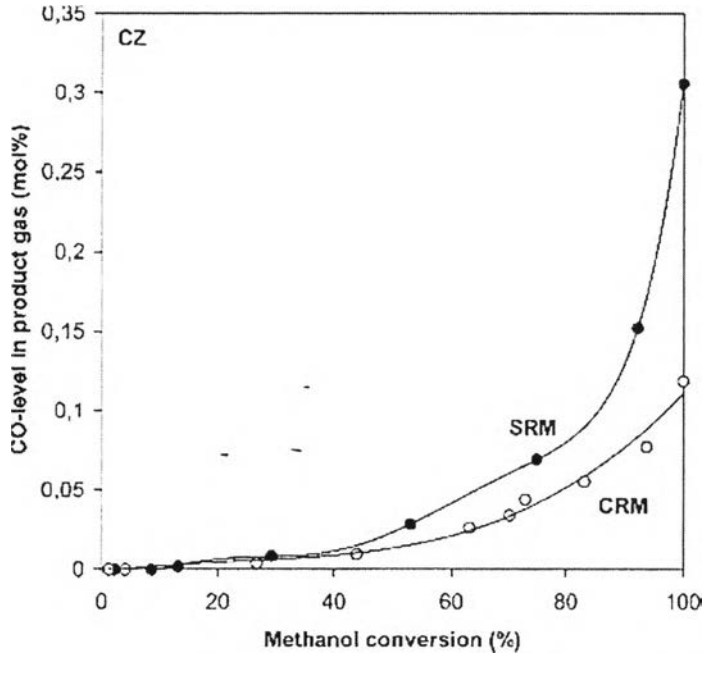

Figure 2.14 CO level in the product gas versus methanol conversion during (●) steam reforming and (○) combined reforming of methanol over catalyst Cu/ZnO (H_2O/CH_3OH = 1.3; O_2/CH_3OH = 0.2 M) (Agrell *et al.*, 2003).

2.3 Gold Catalyst

Gold catalyst has been studied for the reactions that concerned about air pollution. This catalyst exhibited catalytic activity for a wide range of different reactions such as NO_x reduction, CO and CO_2 hydrogenation, NO oxidation, water gas shift reaction, alkene epoxidation, total oxidation of hydrocarbon, and selective oxidation of CO in the presence of hydrogen (Gluhoi *et al.*, 2004). Figure 2.15 shows that supported gold catalyst gave the highest catalytic activity of CO oxidation at very low temperature. The catalytic performances of gold depended on dispersion, supports, and preparation methods. Gold catalysts exhibited high activities and selectivities in many reactions as the particles size is smaller than 5 nm (Haruta, 1997).

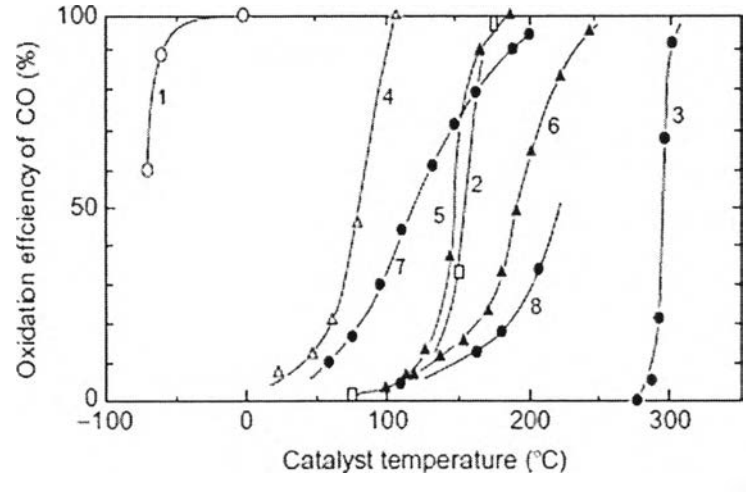

Figure 2.15 CO conversion over various catalysts as a function of temperature (1) Au/α-Fe_2O_3 (Au/Fe = 1/19, co–precipitation, 400 °C), (2) 0.5wt% Pd/γ-Al_2O_3 (impregnation, 300 °C), (3) Au fine powder, (4) Co_3O_4 (carbonate, 400 °C), (5) NiO (hydrate , 200 °C), (6) α-Fe_2O_3 (hydrate, 400 °C), (7) 5 wt% Au/α-Fe_2O_3 (impregnation, 200 °C), and (8) 5 wt% Au/γ-Al_2O_3 (impregnation, 200 °C) (Hutchings and Edwards, 2012).

There are many methods that use to prepare active supported Au catalyst. Each methods gave the different size of Au particles. Deposition–Precipitation (DP) is an efficient method because this method gave the strong interaction between met-

als and the metal oxide supports and gave the small particle as compared to solid grinding (SG), and impregnation (IP) (Shimada *et al.*, 2010). The order of Au particle sizes can be ranged from DP< SG< IP, as shown in Table 2.1.

Table 2.1 Mean diameter of metal particles for 5wt%-Au/CeO_2 (Shimada *et al.*, 2010)

Preparation method	d_{Au}/ nm
IP	53
DP	4.1 ± 1.3
SG	10.6 ± 3.1

To improve the catalytic activity and selectivity to the desired products, the addition of oxidic additives such as Cu, Fe, Ce, Li, and Ti for generating bimetallic catalysts became interesting.

2.4 Bimetallic Catalyst

There are many problems that occur during the reforming process such as low stability due to carbon/coke deposition, sintering of metal (active) phase, oxidation of metal (active) phase, and poor selectivity to desired produces. Therefore, the interesting solution for solving these problems is using of bi- or poly-metallic system which allows to get stable and optimal catalytic performance. The bimetallic catalyst has positive effects that arise from the combination between two metals.

The structures of bimetallic catalyst depend on metal properties, metal-support interaction, atmosphere (oxidant, reductive, presence of water etc.) temperature, etc. Figure 2.16 shows the structure of bimetallic nanoparticles.

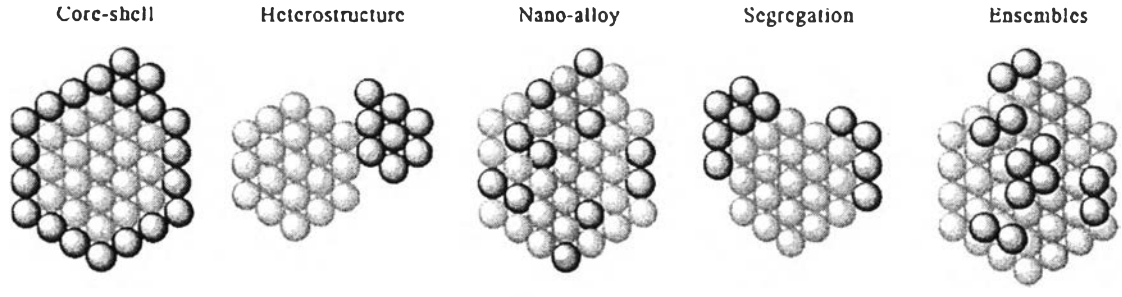

Figure 2.16 Examples of bimetallic nanoparticles structure (Dal Santo *et al.*, 2012).

The principal effects from interactions between two metals (hereinafter indicated as M(n) where n = 1,2,3,... ; and M(1) being the main component) in a bimetallic structure can be classified in 2 phenomena (surface and structural). Surface phenomena were divided in geometric and electronic effects. Geometric effect is the result of surface M(1) atoms dilution by M(2). Electronic effect occurred from the difference in electronic affinity between M(1) and M(2), thus M(1) can suffer an electronic density increase or decrease depending on whether M(2) has a lower or higher electronic affinity. The improvement of bimetallic can be explained by

- The bimetallic catalyst can improve the coke resistance by reducing the size of metallic nanoparticles, hence, lowering the C solubility.
- The bimetallic can enhance the thermal stability of the active metals by increasing its dispersion and/or interaction with support material.
- The bimetallic can enhance the poisoning resistance.

The group VIII metals including Au, Ag, and Cu have the same face center cubic (FCC) crystals structure and similar lattice spacing, hence they can form alloy easily (Liu *et al.*, 2011). Among these metals, copper has attracted much attention due to its cheapness, stability, and catalytic activity. Moreover, the presence of copper in Au–Cu/TiO_2 catalysts preserved the Au particle size during POM reaction. They observed that the mean diameter of this particle about 3 nm was similar for the sample before and after reaction (Ou *et al.*, 2008).

The TPR profile of Au–Cu/TiO_2 catalyst is shown in Figure 2.17. For Au/TiO_2 catalyst, the peak that corresponded to the reduction of oxidized gold spe-

cies was no observed. Cu/TiO_2 catalyst showed 2 reduction peaks. The first peak at 142 °C is attributed to Cu_2O to metallic copper (Cu^0). The second peak at 152 °C is assigned to CuO to metallic copper (Cu^0). TPR profile of bimetallic $Au–Cu/TiO_2$ showed a single reduction peak at lower temperature than monometallic catalyst. This peak is assigned to the reduction of CuO to Cu^0. The explanation of this result is the presence of gold could weaken the bond strength of Cu-O and enhanced the dispersion of CuO into metallic copper.

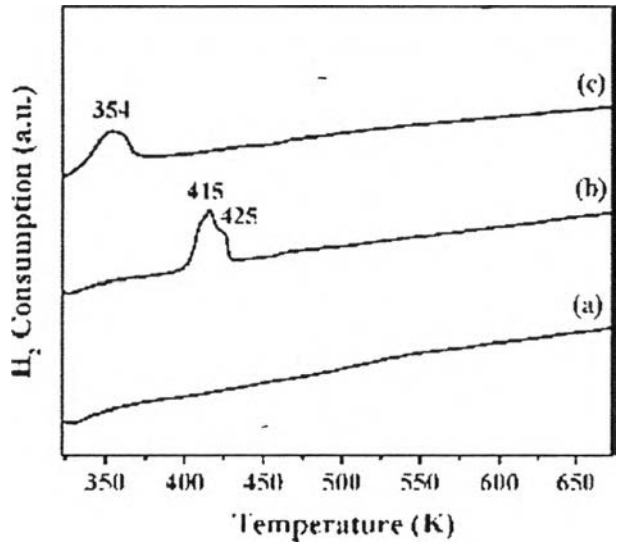

Figure 2.17 TPR profiles of: (a) Au/TiO_2 (2 wt.%); (b) Cu/TiO_2 (2 wt.%); (c) $Au–Cu/TiO_2$ (1-1 wt.%) prepared at pH 7 (uncalcined, dried at 373 K) (Ou *et al.*, 2008).

Pojanavaraphan *et al.* (2013) studied the effect of calcination temperature on the reactive site of $Au–Cu/Ce_{0.75}Zr_{0.25}O_2$ catalysts. This study revealed that the reactive sites of catalysts depended on calcination temperature. At high calcination temperature, the reactive sites of catalysts at the interface between the alloy metals and support were reduced. The decreasing of these sites may be due to copper which covered these sites. Hence, the catalytic activities of catalyst decreased.

The key factor that affected the catalytic activity of bimetallic catalysts is atomic ratio of metals in bimetallic catalysts, as shown in Figure 2.18. The trends of methanol conversion and gas selectivity were increased as the reaction temperature

increased. For bimetallic catalysts, the higher Cu concentration can improve the catalytic activity of reaction. In contrast, Au3Cu1 gave the lowest catalytic activity.

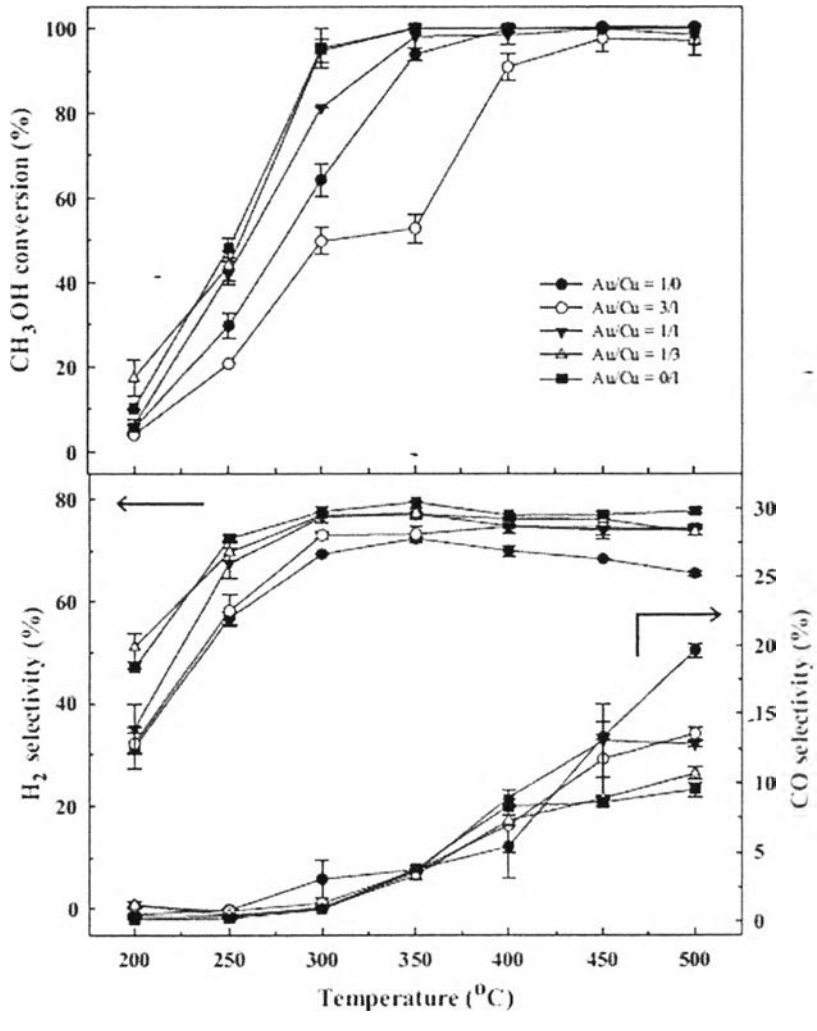

Figure 2.18 Effect of Au/Cu atomic ratio on methanol conversion and product selectivity over 3 wt% Au–Cu/$Ce_{0.75}Zr_{0.25}$ O_2 (reaction conditions: H_2O/CH_3OH, 2/1; calcination temperature, 400 °C) (Pojanavaraphan *et al.*, 2013).

Figure 2.19 shows the catalytic activity of catalyst during POM reaction. The bimetallic catalyst (Au–Cu/TiO_2) showed higher activity and stability than Au/TiO_2 and Cu/TiO_2 catalysts. Moreover, the bimetallic catalyst showed much lower CO selectivity throughout the long operation as compared to other catalysts. The high activity, selectivity, and stability of bimetallic catalyst corresponded to the

charge transfer in metal–metal species which increased the availability of reactive oxygen.

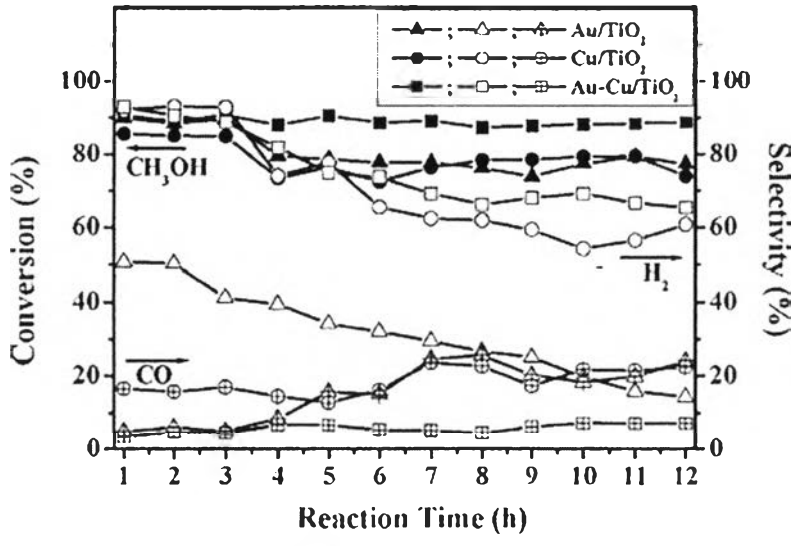

Figure 2.19 Catalytic performance of Au/TiO_2, Cu/TiO_2, and $Au–Cu/TiO_2$ catalysts for CH_3OH conversion, H_2 selectivity, and CO selectivity for POM (Ou *et al.*, 2008).

2.5 Supports

Cerium oxide or Ceria (CeO_2) is widely used as a promoter for automotive exhaust catalyst due to its activity: stabilization of the metal dispersion, promotion of the water gas shift reaction, and enhanced oxygen storage and released by shifting between Ce^{4+} and Ce^{3+} under reducing conditions (Equation 2.22). Ceria was focused to be used in the interaction with small molecules such as hydrogen, carbon monoxide, oxygen, and nitric oxide (Alessandro, 1996).

$$CeO_2 \leftrightarrow CeO_{2-x} + x/2\ O_2 \qquad (2.22)$$

Due to its high oxygen storage capacity (OSC), ceria was used to produce the three way catalyst (TWC), which is proper for using in vehicle applications. Ceria had the fluorite structure that consisted of a cubic close-packed array of metal atoms with all tetrahedral holes filled by oxygen (Trovarelli, 1996). When ceria was

treated in a reducing atmosphere, it forms a series of discrete compositions which composed of oxygen vacancies. However, it can remain in its fluorite crystal structure and ready to oxidize to the CeO_2 form again.

Nevertheless, the properties of ceria are lost as the reaction temperature increases. The fast deactivation of catalysts attributed to the blockage of the active sites by carbonate and/or formate during WGS reaction. The cause of this problem came from oxygen insufficiency that stimulated the formation of carbonate and formate species on oxide supports (Zhang *et al.*, 2011). To solve this problem, the incorporation of foreign cations ($M^{\delta+}$: Si^{4+}, Th^{4+}, Zr^{4+}, Y^{3+}, La^{3+}, Sc^{3+}, Mg^{2+}, Ca^{2+}, and Cu^{2+}) can improve the stability, catalytic activity, textural features and OSC of ceria (Pijolat *et al.*, 1995). Among the various types of cations, zirconium oxide or zirconia (ZrO_2) has attracted much attention due to higher thermal stability and activity than pure ceria (Figure 2.20). The addition of ZrO_2 into CeO_2 also formed solid solution and increased the stability of catalyst. Due to the mixed oxide more acid than pure ceria, therefore, carbonate and formate species, which preferred to adsorb on the surface of basic oxide, cannot adsorb like before (Vindigni *et al.*, 2012). Moreover, this combination can control the specific surface area (SSA) of catalyst. In pure CeO_2 catalysts, the %decrease of SSA is higher than mixed oxide catalyst. This may be due to the ZrO_2, which reduced easily, stabilized the texture of the binary supports (Kambolis *et al.*, 2010).

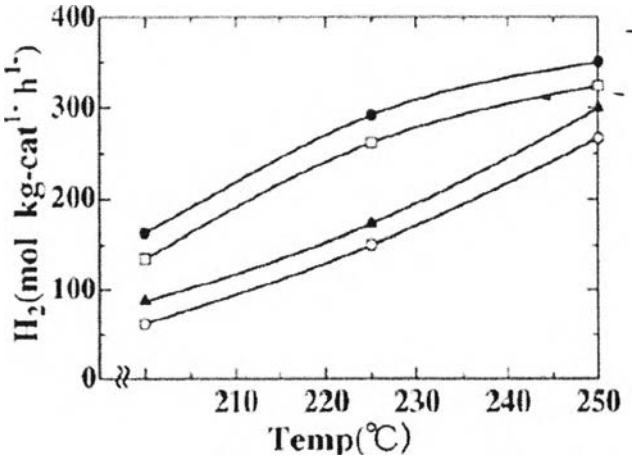

Figure 2.20 Effect of the additives on the activity of CuO/CeO_2: (●)ZrO_2; (□) Al_2O_3; (▲) Y_2O_3; (○) none (Oguchi *et al.*, 2005).

XRD patterns were used to study the effect of the incorporation of CeO_2 with ZrO_2 (Figure 2.21). When ZrO_2 was mixed with CeO_2, the peak intensity decreased, broadened and shifted to higher theta value. This is due to zirconium cations that replaced cerium cations in the lattice structure. In addition, as the ZrO_2 increased up to 59%, the diffraction peaks that corresponded to ZrO_2 were not observed. This indicated that the formation of solid solution might occur.

Ni/CeO_2–ZrO_2 catalyst was studied in OSRM reaction (Pérez-Hernández *et al.*, 2011). The highest catalytic performance was obtained from Ni/Ceria-rich catalyst which exhibited stable performance during 2 cycles of reaction without deactivation and the highest methanol conversion. However, this catalyst does not provide the high H_2 selectivity as compared to Ni/ZrO_2-rich catalyst.

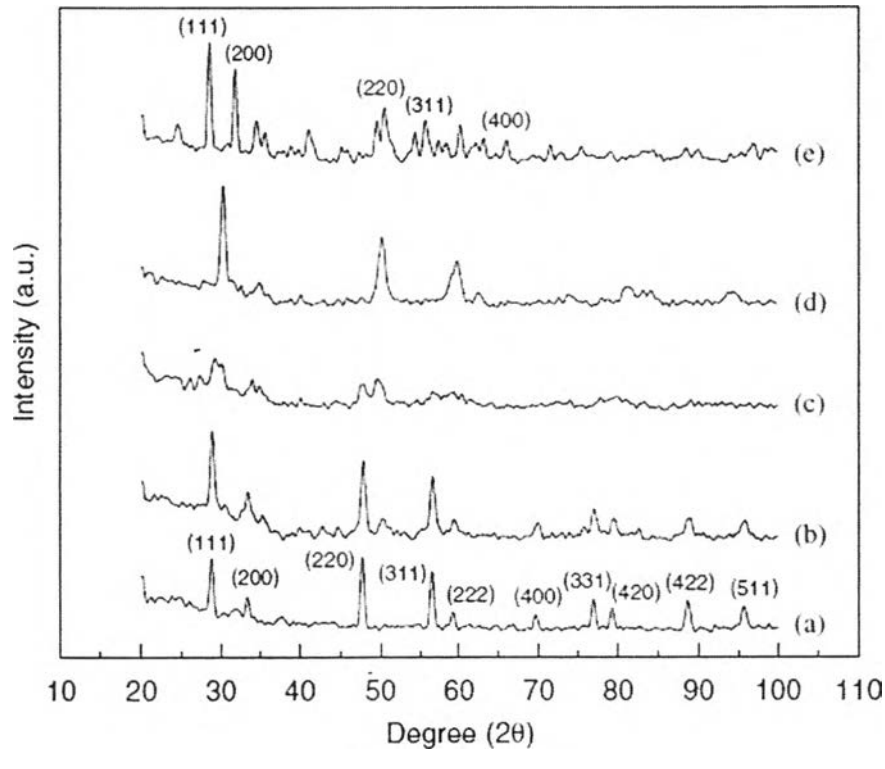

Figure 2.21 XRD patterns of CeO_2, ZrO_2, and CeO_2–ZrO_2 mixed oxide (a) CeO_2, (b) $Ce_{0.74}Zr_{0.26}O_2$, (c) $Ce_{0.41}Zr_{0.59}O_2$, (d) $Ce_{0.16}Zr_{0.84}O_2$, (e) ZrO_2 (Biswas and Kunzru , 2007).

Pojanavaraphan *et al.* (2013) studied the catalytic activities of 3 wt%Au/$Ce_{1-x}Zr_xO_2$ in steam reforming of methanol (Figure 2.22). They found that the activity was improved by the Zr incorporation. The orders of catalyst from the highest to lowest activity are as follows: Au/$Ce_{0.75}Zr_{0.25}O_2$> Au/$Ce_{0.5}Zr_{0.5}O_2$> Au/$Ce_{0.25}Zr_{0.75}O_2$.

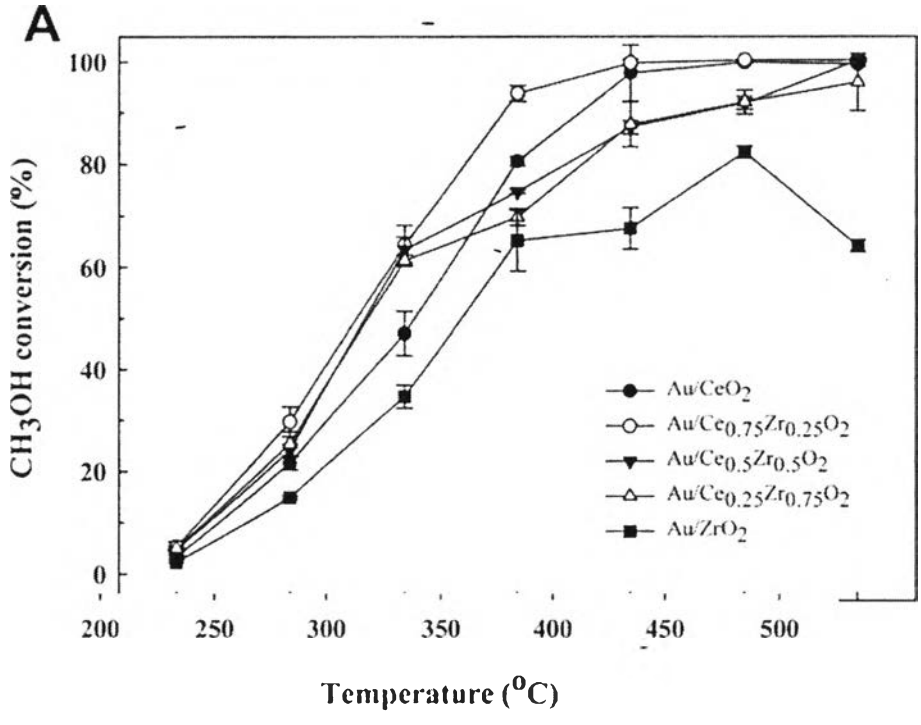

Figure 2.22 Catalytic activities of 3wt%Au/$Ce_{1-x}Zr_xO_2$ (prepared by co–precipitation method) (Pojanavaraphan *et al.*, 2013).

All of these documents are the motivation in this work to study the effect of mixed support preparation (CeO_2–ZrO_2), bimetallic (Au–Cu) atomic ratio, calcination temperature, steam-methanol molar ratio, oxygen-methanol molar ratio, and reaction temperature on the catalytic activity of Au–Cu/CeO_2–ZrO_2 catalyst for OSRM.